

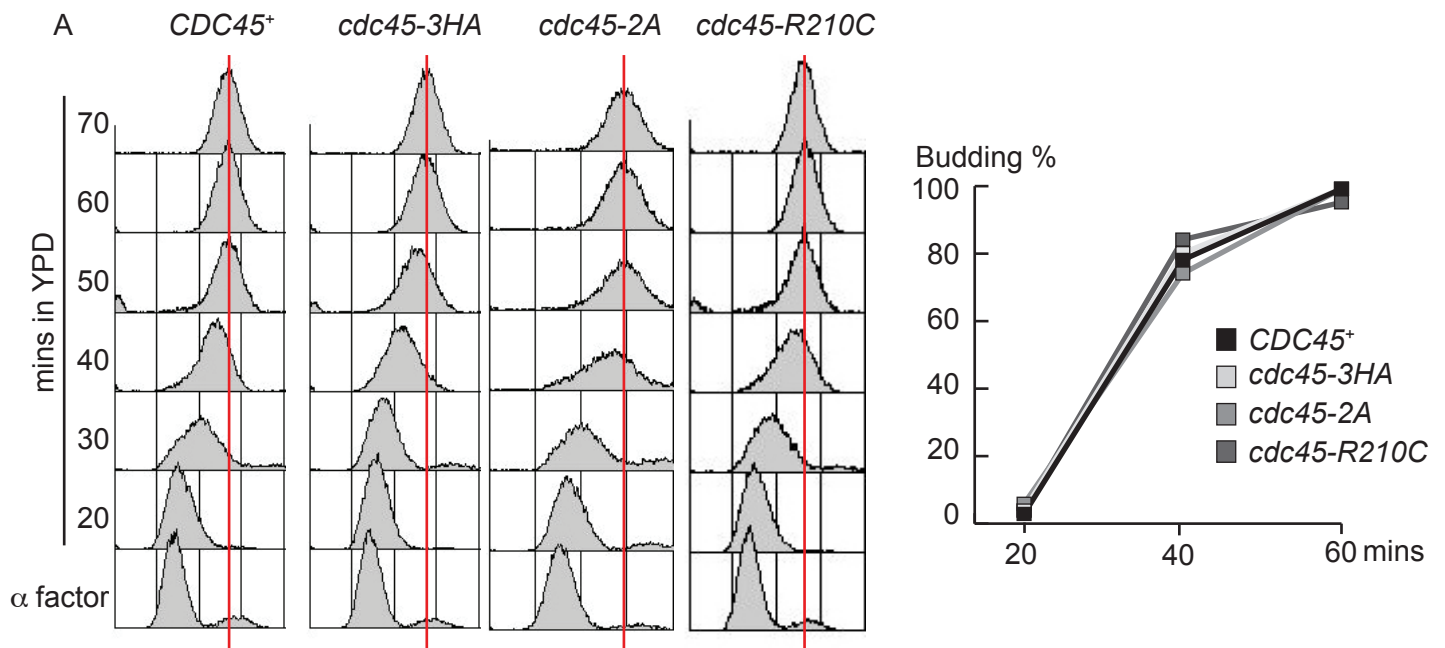
Molecular Cell, Volume 73

Supplemental Information

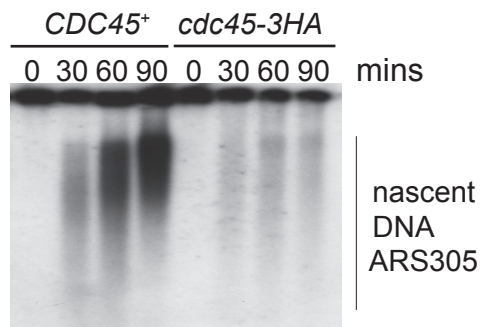
**Helicase Subunit Cdc45 Targets the Checkpoint
Kinase Rad53 to Both Replication Initiation
and Elongation Complexes after Fork Stalling**

Geylani Can, Anastasia Christine Kauerhof, Dominik Macak, and Philip Zegerman

Figure S1



B alpha-factor → 200mM HU



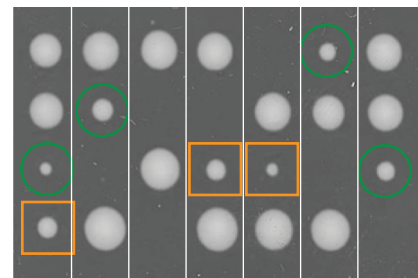
C *sml1Δ cdc45-3HA* x *sml1Δ rad53Δ*

n=64 genotype	expected frequency	actual frequency
<i>sml1Δ cdc45-3HA RAD53</i> ⁺	25%	24%
<i>sml1Δ cdc45-3HA rad53Δ</i>	25%	0%

D *cdc45-2A* x *sml1Δ rad53Δ*

n=68 genotype	expected frequency	actual frequency
<i>sml1Δ RAD53</i> ⁺ <i>cdc45-2A</i>	12.5%	16%
<i>sml1Δ cdc45-2A rad53Δ</i>	12.5%	12%

□ *sml1Δ rad53Δ*
○ *sml1Δ cdc45-2A rad53Δ*



E Hydroxyurea in S-phase

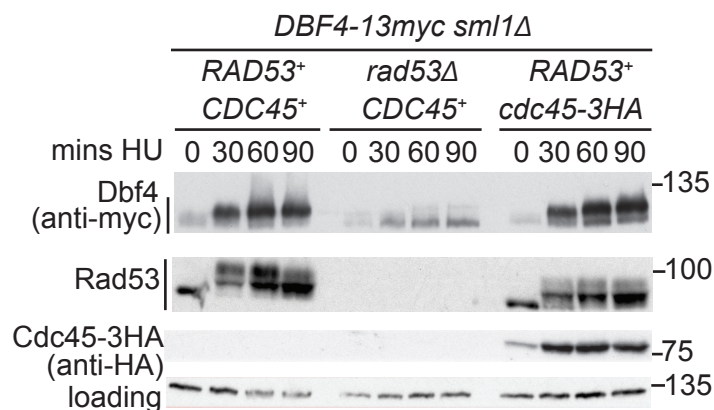
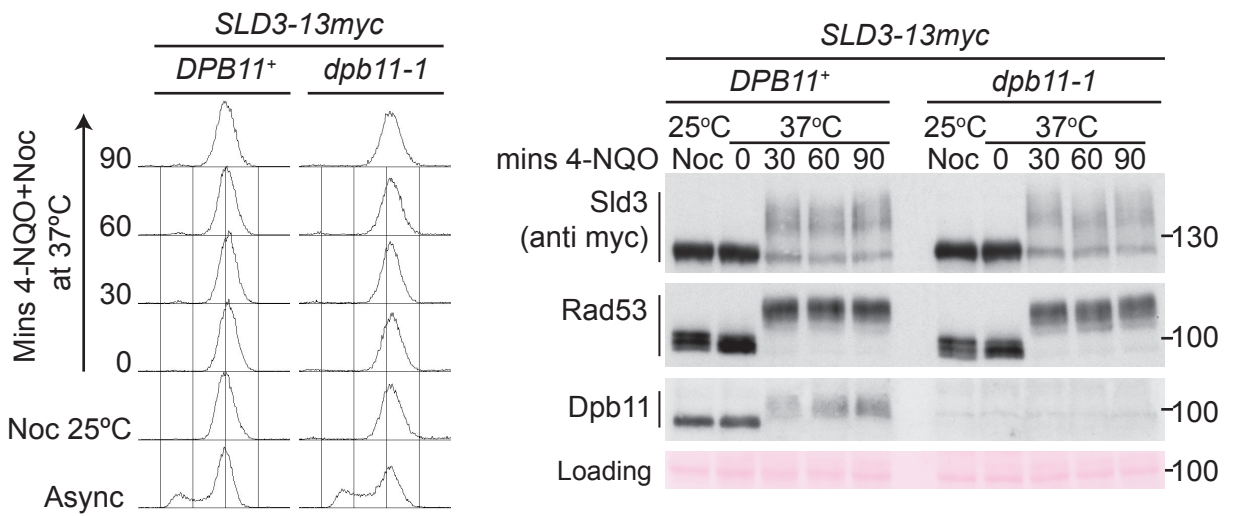
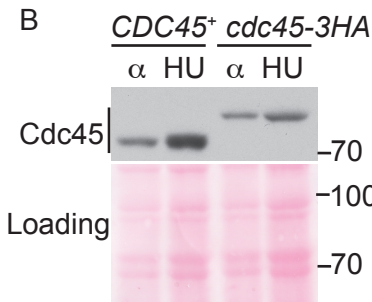


Figure S2

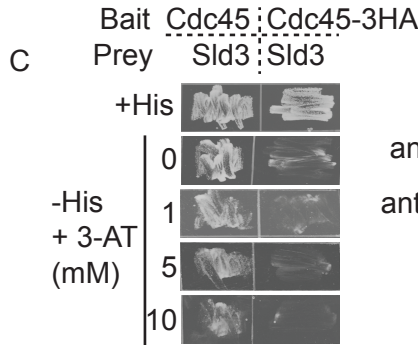
A



B



C

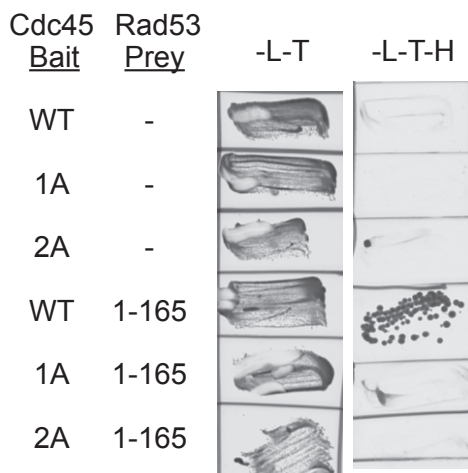


The Cdc45 2A mutant has both T189 and T195 mutated to alanine

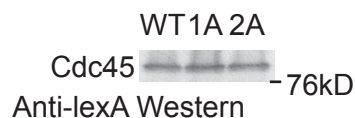
D

S.cerevisiae 156 KEAYYKLLLELD---EESGDDELSGDENDN-----NGGDDEATDADEVTDDEEE
C.albicans 173 KEAYNVLVEMSDSEDEDEDEGHNQNGHAD-----DDQEGDKTDADDENDESSV
S.bayanus 156 KAAYYKLLLELENGREQDGDGGLSDDDDDDDDDDNDGEDEM~~TDAD~~EAADEGED
S.kluyveri 153 REAYYKLMLELEDEQNS~~ESD~~GDPEEND~~TEED~~SDEKDSGDEDSDDDFPGKRRVNO
Y.lipolytica 144 LVAYYNWLN~~DMSAEELDALSDLEDEGD~~DDDDDDDDQIHKRNGHHTNTVDDNDSD

E



1A = T189A
2A = T189A / T195A



F

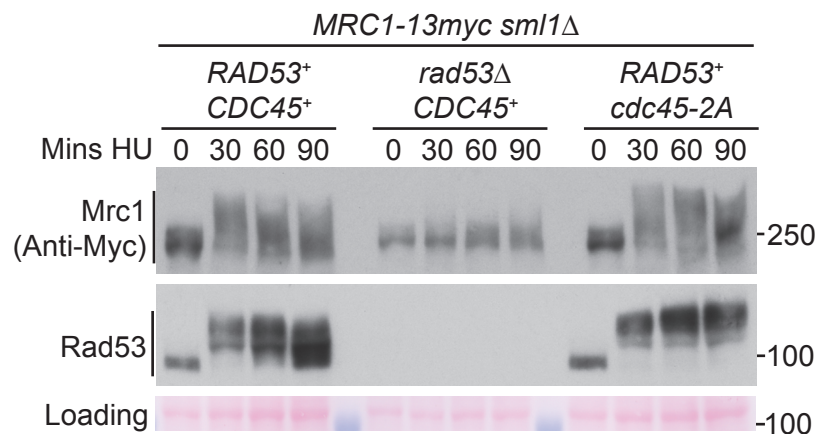


Figure S3

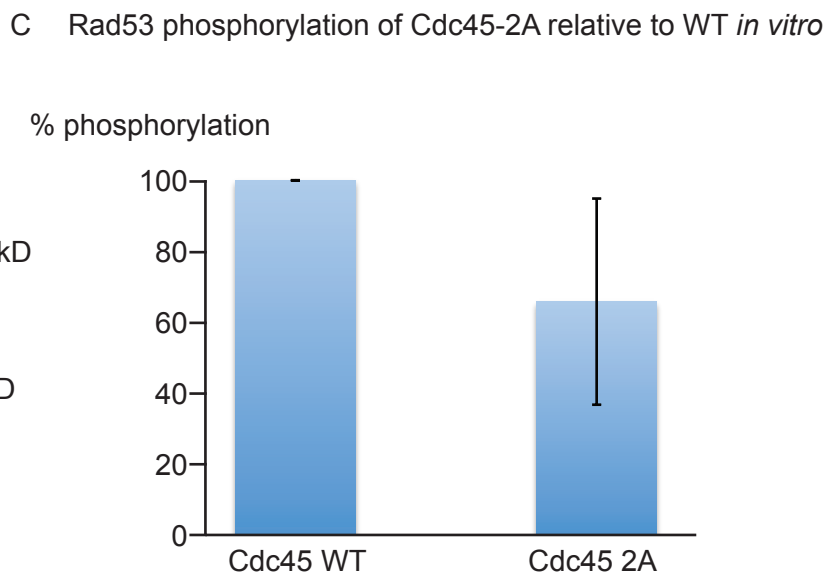
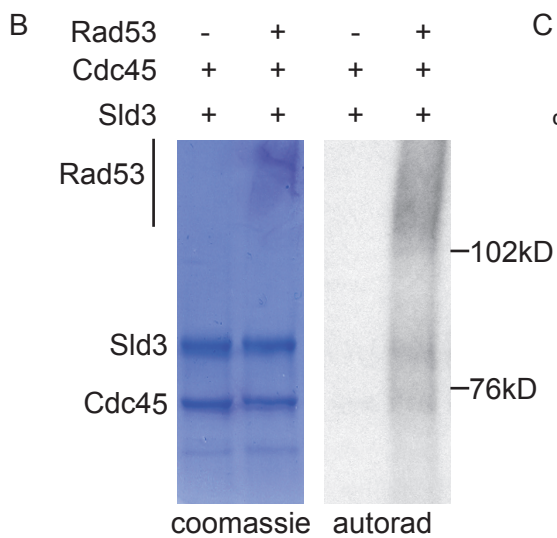
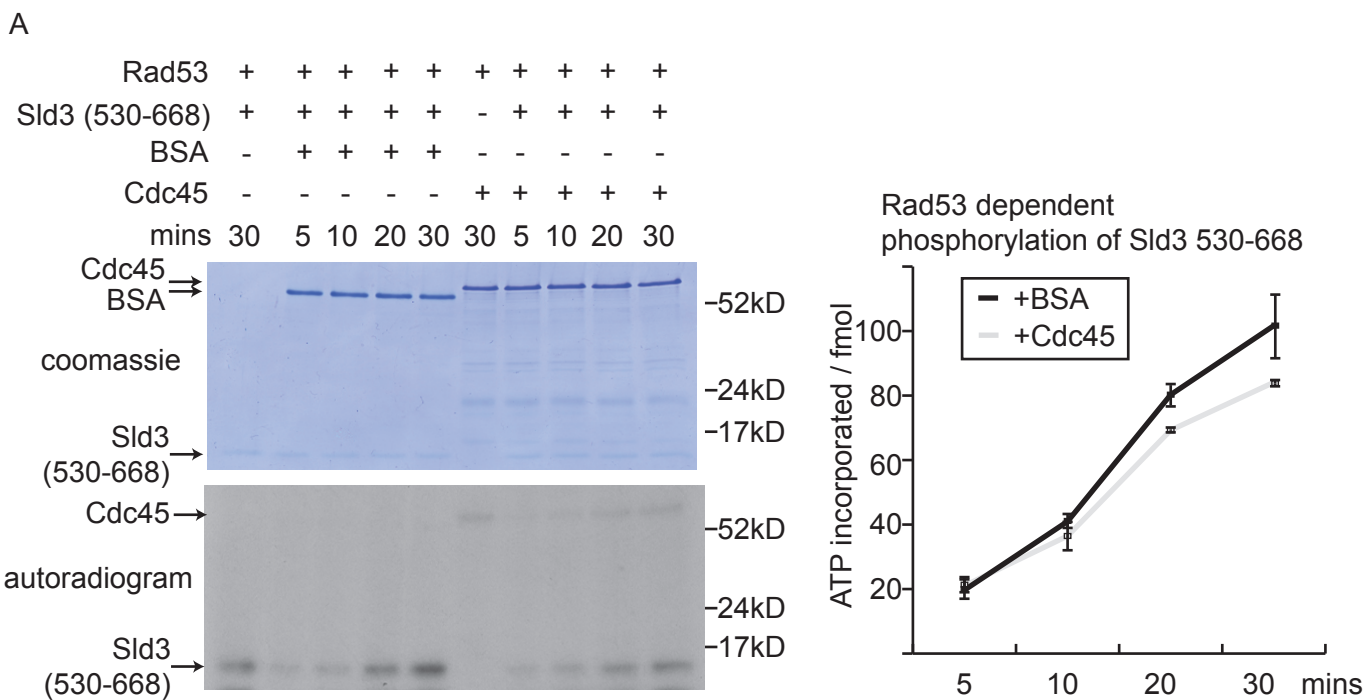
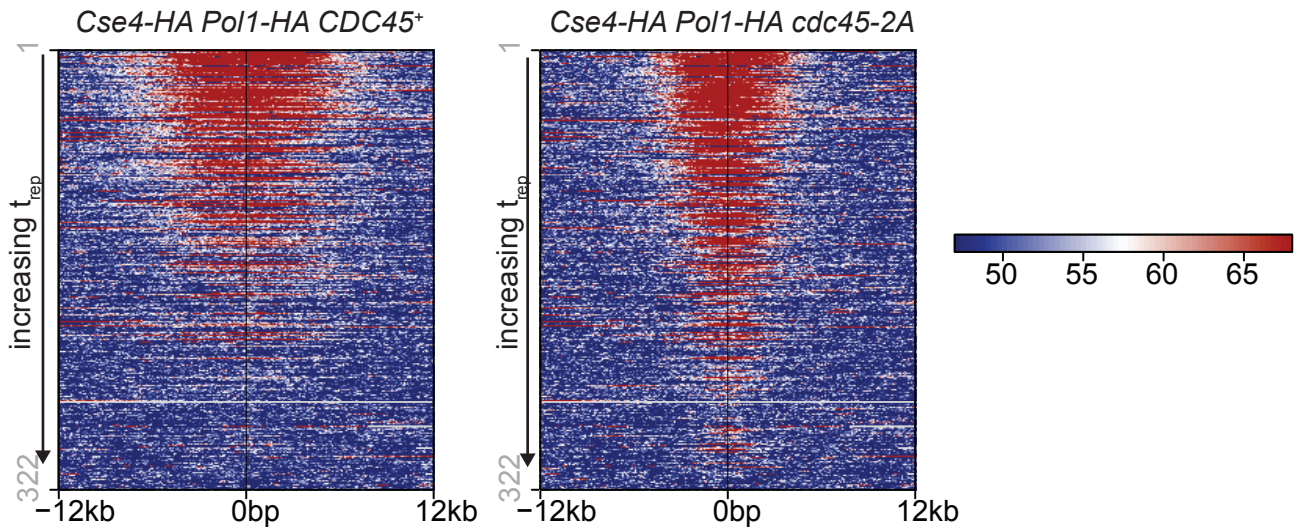
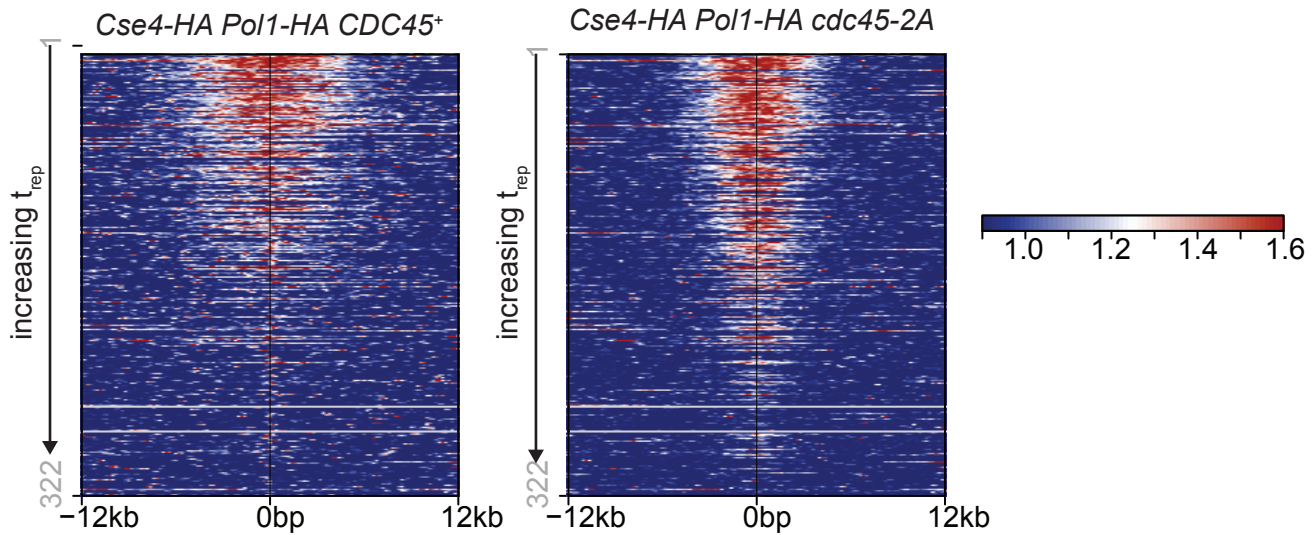


Figure S4

A. ChIP of Pol1 at 322 origins sorted by tREP α factor \rightarrow HU 60mins



B. Copy number analysis at 322 origins sorted by tREP α factor \rightarrow HU 60mins



C. Copy number analysis in *sld3-A dbf4-A* strains α factor \rightarrow HU 60mins

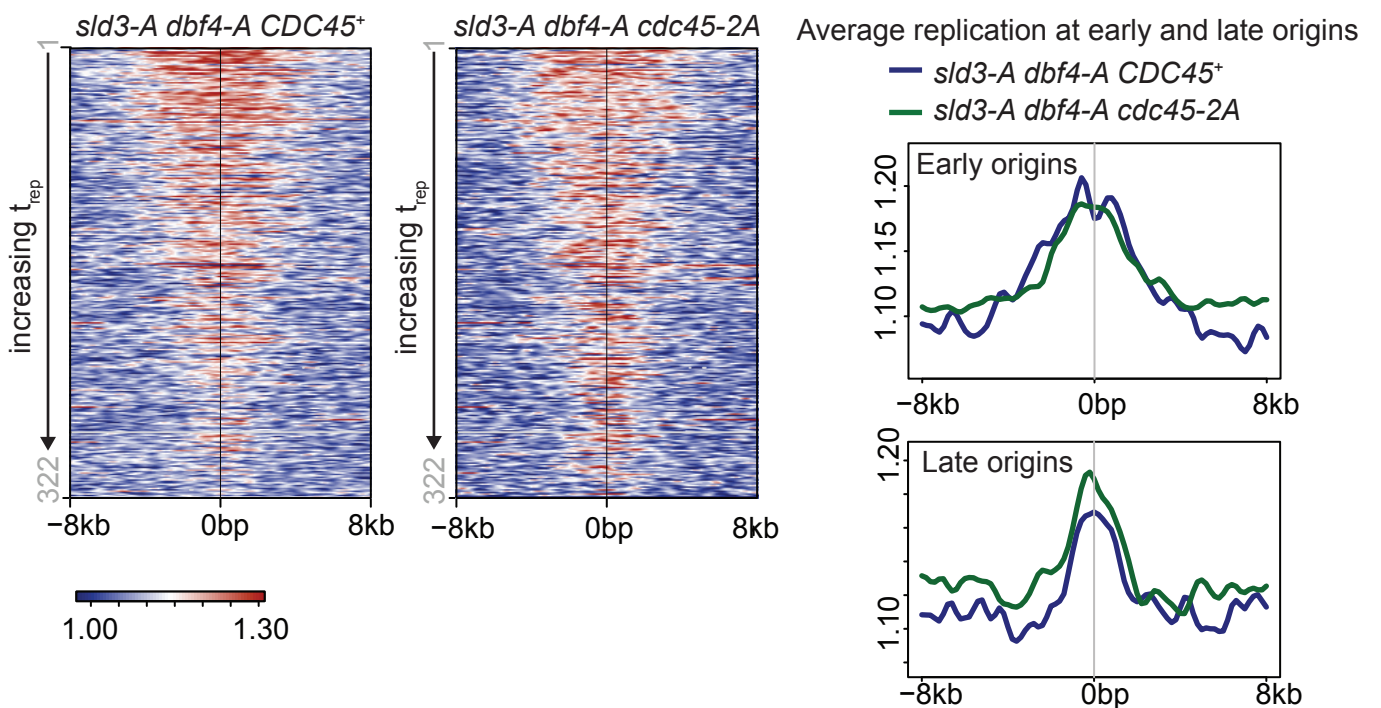
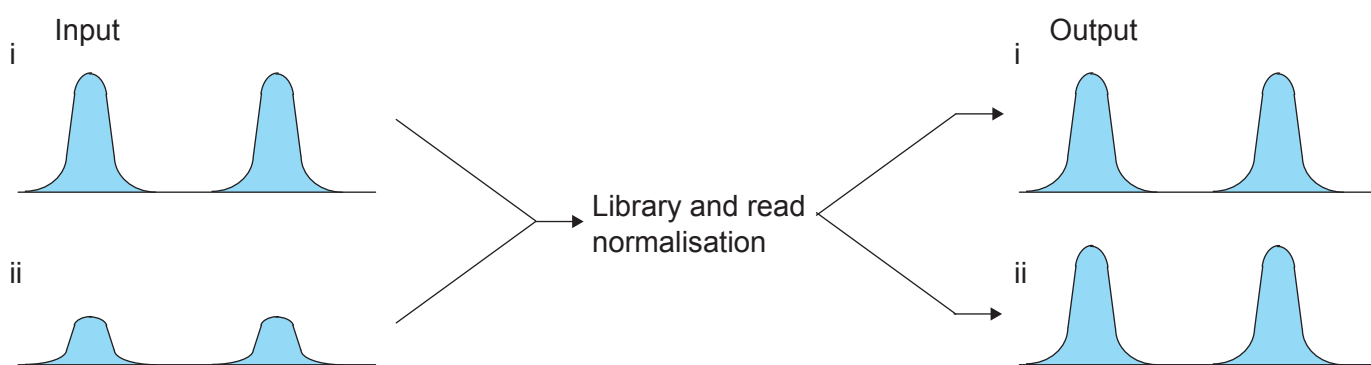
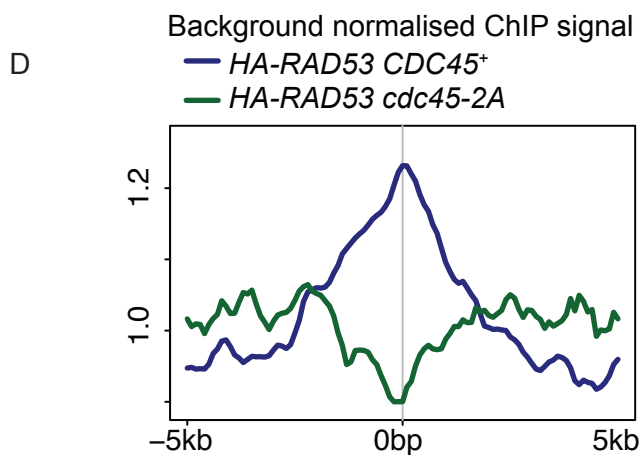
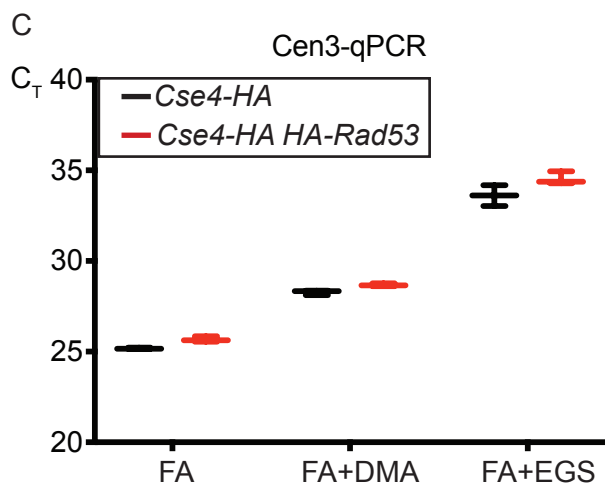
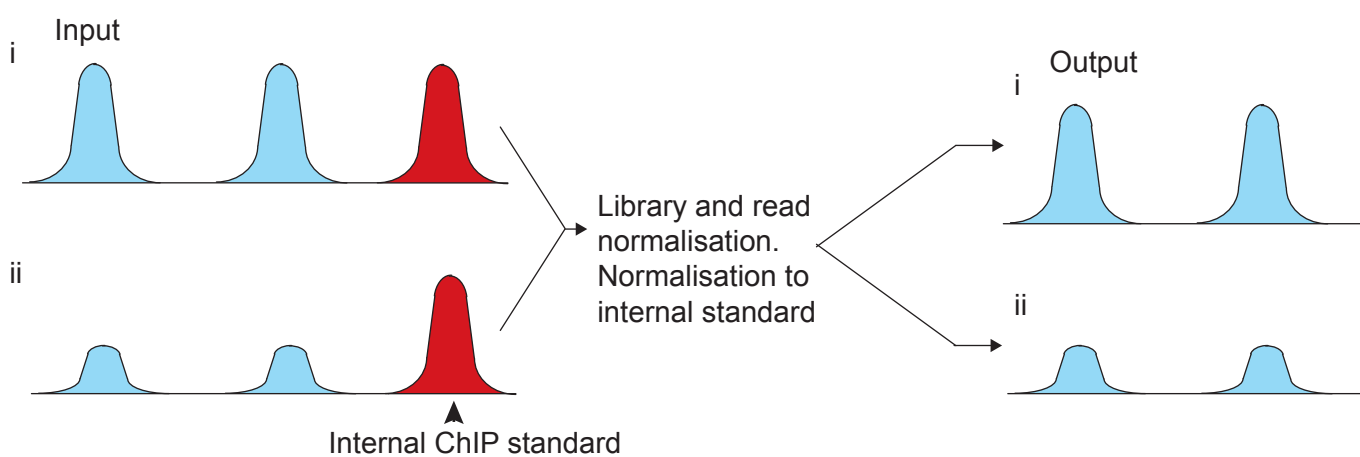


Figure S5

A ChIP signal - no internal standard



B ChIP signal - using internal standard



E Anti HA ChIP from *HA-Rad53 Cse4-HA sld3-A dbf4-A*

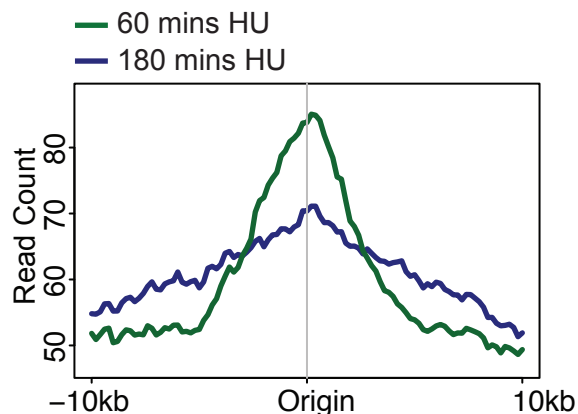


Figure S6

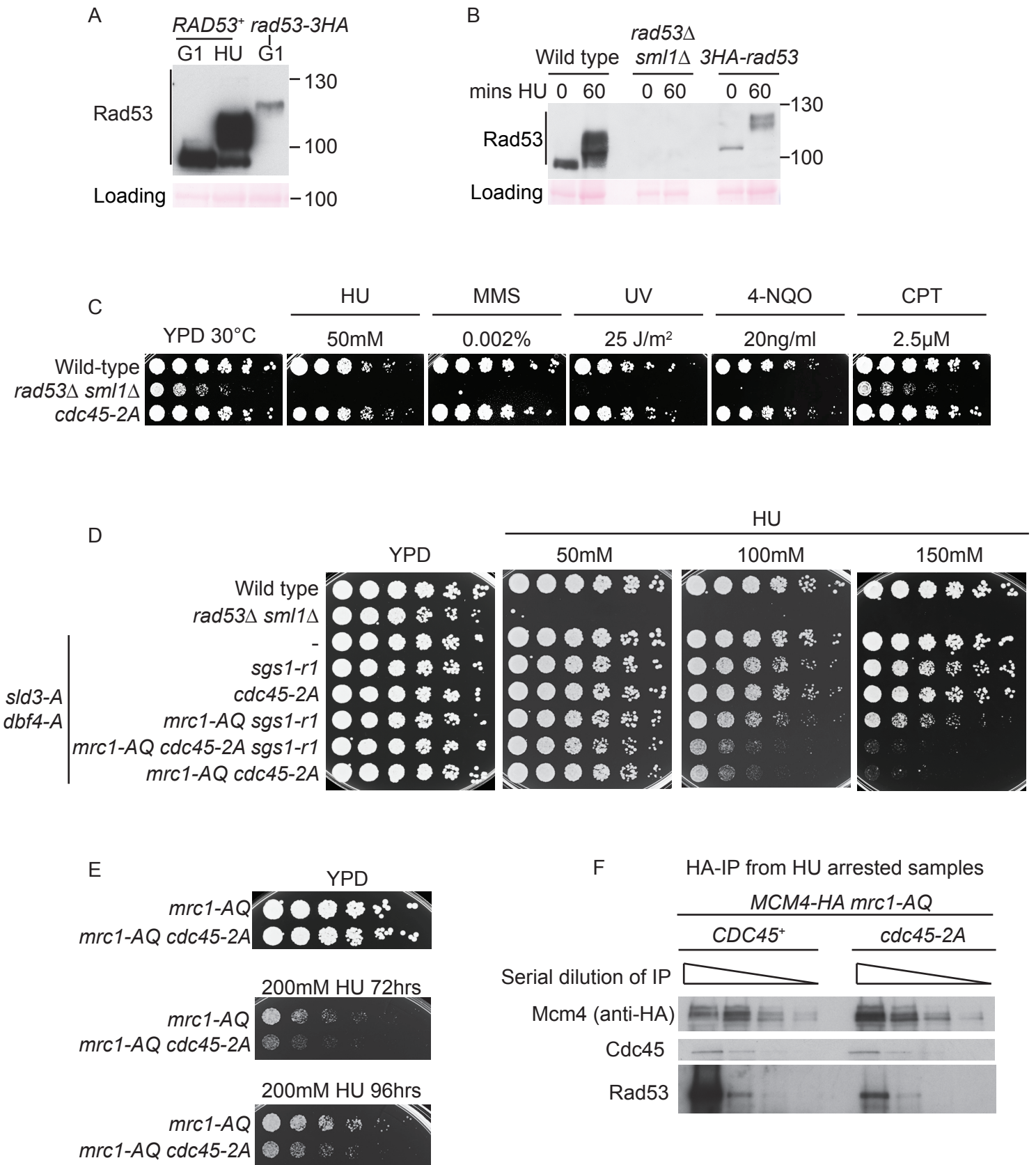
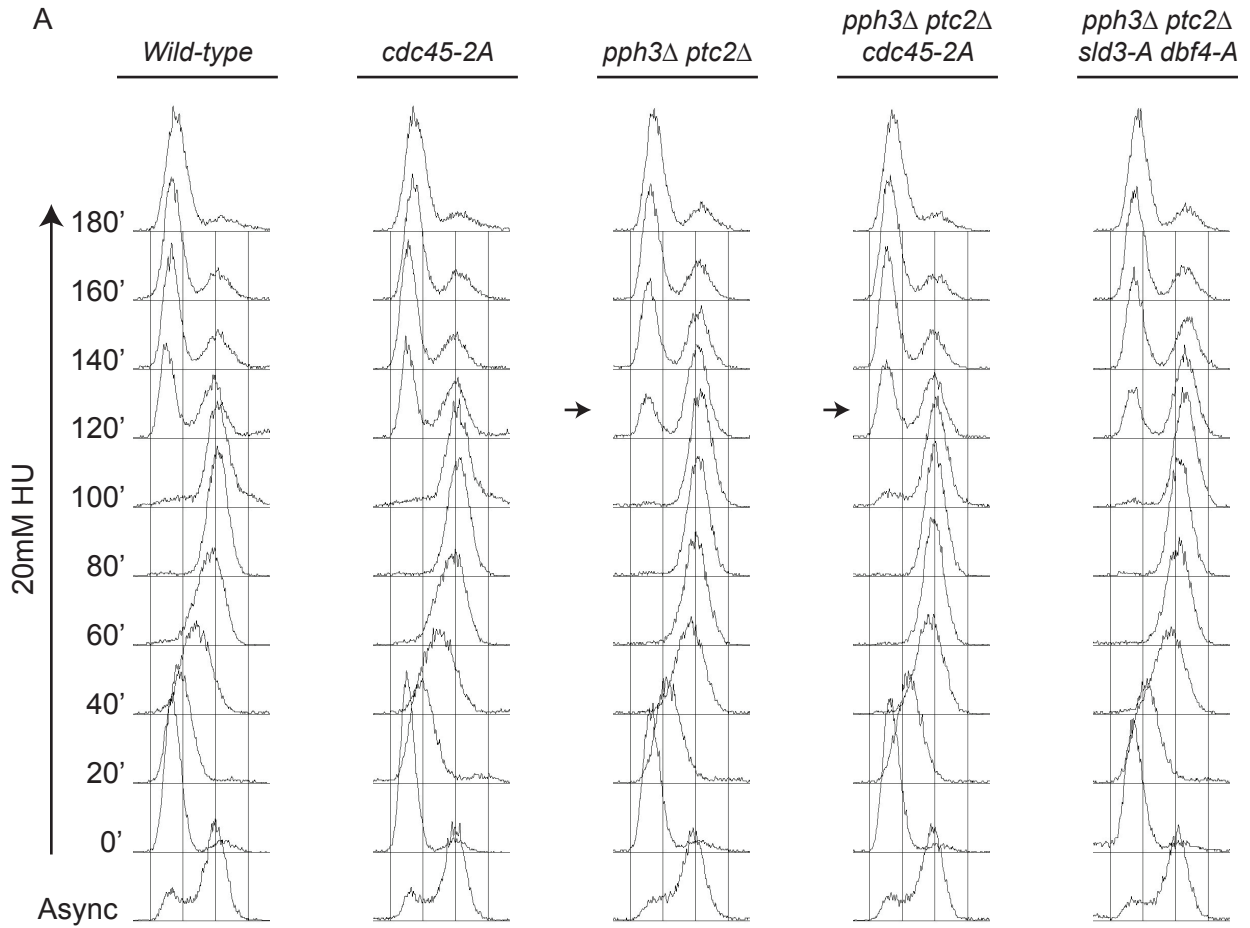
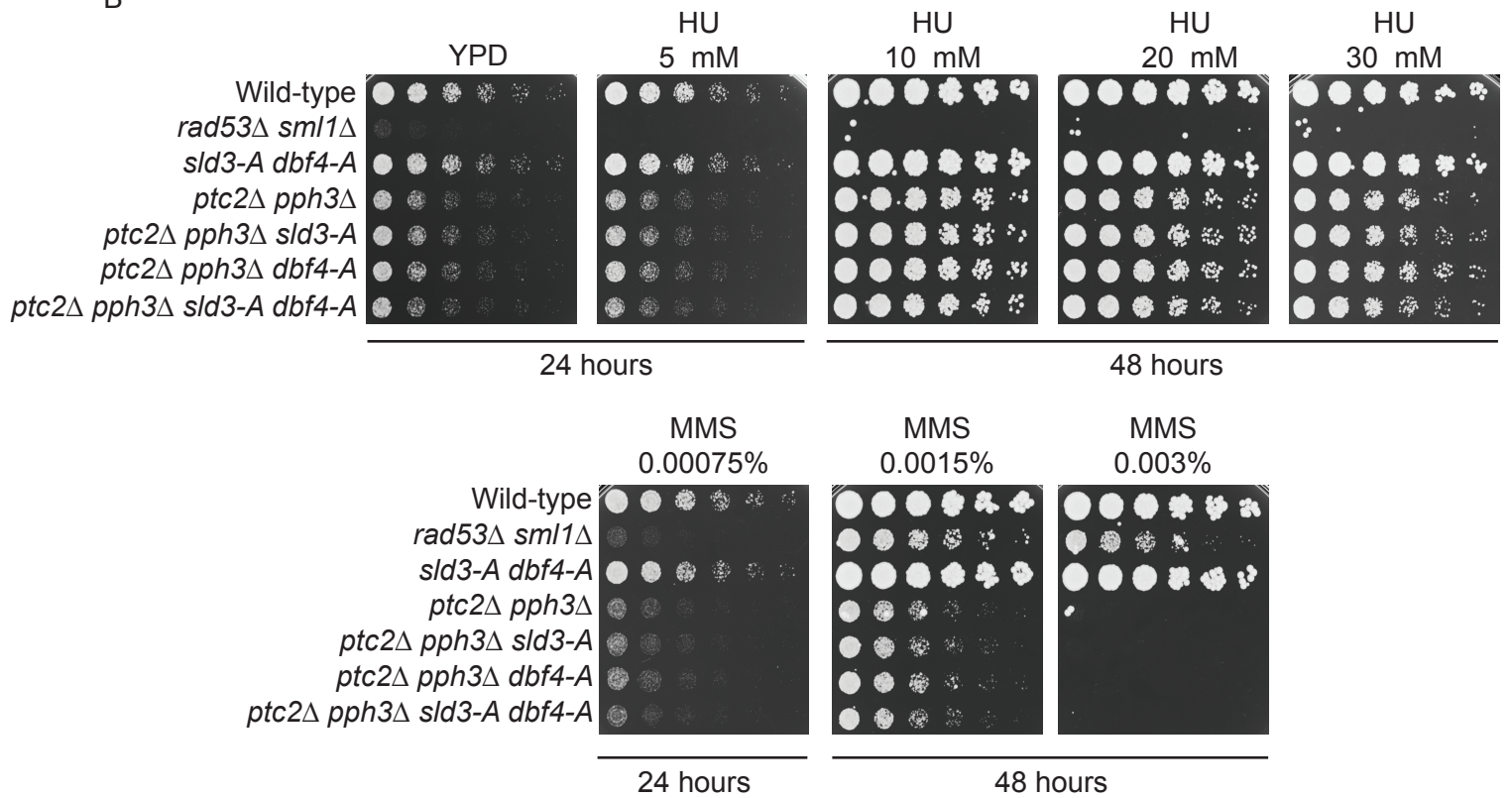


Figure S7
A



B



Supplementary figure legends

Figure S1. Phenotypes of Cdc45 mutants, Related to Figure 1 and 2.

A) Flow cytometry (left) and budding index (right) of the indicated Cdc45 mutants released from alpha factor into S-phase at 25°C. The red line indicates the position of the 2N DNA content.

B) Autoradiogram of a Southern blot of an alkaline gel of replication intermediates from strains released from alpha factor into 200mM HU. Southern blot was probed for ARS305.

C) Table of the expected and actual frequency of genotypes from the indicated genetic cross.

D) as C) (left) and image of tetrads (right) indicating the growth of *rad53* null colonies with and without *cdc45-2A*. Dead spores are *rad53* null and *SML1*⁺.

E) Western blots of the indicated yeast strains, released from alpha factor (0) into 200mM HU. Loading control is a non-specific band from the HA western blot.

Figure S2. Effect of Cdc45 mutants on the interaction with Sld3 or Rad53, Related to Figure 1 and 2.

A) Flow cytometry (left) and Western blots (right) of the indicated strains arrested at 25°C in nocodazole, then shifted to 37°C before addition of 10µg/ml 4-NQO.

B) Anti-Cdc45 Western blot of the indicated yeast strains, released from alpha factor (α) into 200mM HU for 60 minutes.

C) Yeast-two hybrid growth assay (left) between full length Cdc45 and Sld3 on non-selective (+His) and selective medium (-His). 3-AT is 3-aminotriazole. Right, Western blot of yeast-two hybrid fusion proteins as indicated.

D) Alignment of unstructured acidic loop region of Cdc45 from Saccharomycotina yeast species. Potential FHA interaction TxxD motifs are underlined.

E) Yeast-two hybrid growth assay between full length Cdc45 and Rad53 FHA1 (1-165) on non-selective (-L-T) and selective medium (-L-T-H). WT corresponds to wild type, 1A is T189A, 2A is T189A/T195A. Bottom, Western blot of yeast-two hybrid fusion proteins as indicated.

F) As Figure 1C.

Figure S3. Rad53 is not activated by Cdc45 non-specifically and phosphorylates Cdc45 at T189/T195 *in vitro*. Related to Figure 4.

A) Kinase assay (left) with Rad53, Sld3 C-terminus (530-668) and either BSA or Cdc45. Sld3, Cdc45 and BSA were in 25 fold excess over Rad53. Top; Coomassie stained gel, Middle; autoradiogram. (right) Quantitation of the kinase assay. Error bars are standard deviation, n=3.

B) As A), demonstrating the dependence of Sld3 and Cdc45 phosphorylation on Rad53.

C) Quantitation of the Rad53 phosphorylation of Cdc45 wild type (WT) and Cdc45 T189A/T195A (2A). Cdc45 WT phosphorylation was set to 100%. Error bars are standard deviation, n=4.

Figure S4. Cdc45-2A affects replisome position. Related to Figure 5.

A) Anti-HA (Pol1) CHIP of the indicated strains released from alpha factor (G1) into 200mM HU for 60 mins. Data is presented as a heatmap of sequencing reads normalised to the reads from 500bp either side of all yeast centromeres. The map is centred on 322 of the yeast origins, arranged by increasing t_{rep} .

B) DNA sequencing reads for the input samples before HA-IP from A) were quantified to derive DNA copy number genome-wide. Data was normalised to a G1 sample and is represented as a ratio of S/G1.

C) Left heatmaps as B). Right. Data is represented as a graph of the average signal from 322 origins, centred on the origin. The graphs, separated into early and late firing origins (161 each), demonstrates that average replication amount/position is very similar between strains containing *sld3-A dbf4-A*.

Figure S5. Normalisation of ChIP-seq signal using Cse4-HA. Related to Figure 5.

A) Read/library normalisation from ChIP-seq data can result in distortion of peak heights between samples.

B) Use of internal standard (red) for normalisation can allow direct comparison of peak heights between samples.

C). qPCR of centromeric locus Cen3 from anti-HA ChIP from the indicated strains. ChIP was performed with 3 different crosslinking procedures; formaldehyde alone (FA), FA + dimethyl adipimidate (DMA) or FA + ethylene glycol disuccinate (EGS). Error bars are standard deviation, n=3.

D) Data from Figure 5A, normalised to background reads at an unreplicated genomic locus instead of the Cse4-HA signal around centromeres.

E) Graph representing average signal at 322 origins from anti-HA ChIP reads from strain *HA-Rad53 Cse4-HA sld3-A dbf4-A*. Data was normalised to the Cse4-HA signal, using 500bp either side of all yeast centromeres.

Figure S6. Growth defect of *cdc45-2A* is not exacerbated by the *sgs1-r1* mutant. Related to Figure 6.

A) Western blot of C-terminally tagged Rad53.

B) Western blot of N-terminally tagged Rad53.

C) Growth assay of the indicated strains.

D) as C), the bottom 6 strains are all *sld3-A dbf4-A*.

E) As C).

F) Anti Mcm4-HA IP as in Figure 5D. The IPs were serially diluted 2-fold to give an indication of the relative difference in Rad53-replisome interaction between Cdc45 wild type and *cdc45-2A* strains.

Figure S7. Cdc45-2A suppresses the cell cycle delay of *pph3Δ ptc2Δ* strains.

Related to Figure 6.

A) Flow cytometry of the indicated strains released from alpha factor (0) into 20mM HU. Arrows highlight the faster progression through the cell cycle of the *pph3Δ ptc2Δ cdc45-2A* strain.

B) Growth assay of the indicated strains.